

Contents lists available at [ScienceDirect](https://www.sciencedirect.com)

Forest Ecology and Management

journal homepage: www.elsevier.com/locate/foreco

Model analysis of forest thinning impacts on the water resources during hydrological drought periods

Hiroki Momiyama^{a,*}, Tomo'omi Kumagai^{a,b,c}, Tomohiro Egusa^{a,d}^a Graduate School of Agricultural and Life Sciences, The University of Tokyo, Tokyo, Japan^b Institute for Space-Earth Environmental Research, Nagoya University, Nagoya, Japan^c Water Resources Research Center, University of Hawai'i at Mānoa, Honolulu, USA^d Faculty of Agriculture, Shizuoka University, Shizuoka, Japan

ARTICLE INFO

Keywords:

Forest management
 Coniferous plantation
 Interception
 TOPMODEL
 Low-flow
 Stochastic rainfall model

ABSTRACT

In Japan, there has recently been an increasing call for forest thinning to conserve water resources from forested mountain catchments in terms of runoff during prolonged drought periods of the year. How their water balance and the resultant runoff are altered by forest thinning is examined using a combination of 8-year hydrological observations, 100-year meteorological data output that is generated using a stochastic model, and a semi-process-based rainfall-runoff model. The rainfall-runoff model is developed based on TOPMODEL assuming that forest thinning has an impact on runoff primarily through an alteration in canopy interception. The main novelty in this analysis is that the availability of the generated 100-year meteorological data allows the investigations of the forest thinning impacts on mountain catchment water resources under the most severe drought conditions. The model is validated against runoff observations conducted at a forested mountain catchment in the Kanto region of Japan for the period 2010–2017. It is demonstrated that the model reproduces temporal variations in runoff and evapotranspiration at inter- and intra-annual time scales, and the flow duration curves were well reproduced. On the basis of projected flow duration curves for the 100-year, despite the increase in an annual total runoff with thinning, low flow rates (the flows within the range of >70% time exceedance) in both dry and normal years (the years in which low flow are the lowest and 50th the lowest) were impacted by the forest thinning to a lesser extent. Simulations also showed that low flows would increase more with higher catchment water retention capacity, and higher catchment water retention capacity would enhance the forest thinning effect on increasing available water resources. This study would be helpful in planning for better forest management considering runoff from forested catchments.

1. Introduction

Forested headwaters supply water resources to billions of people at a global scale, which are derived from a balance between runoff from the catchment and water use by vegetation (McDonnell et al., 2018). Thus, it has been expected that some forest management has the potential to aid effective use of water yield from the headwater catchment (Andréassian, 2004; Grant et al., 2013). In Japan, forests cover ~70% of the total land area with the majority situated in the mountain region, and the forested headwaters play a significant role in supplying water to lowlands. However, water shortages still occur around Japan, and climate change causes drought risks to be more severe because of the increasing

frequency of dry days and reduction in snowfall (Ministry of Land, Infrastructure, Transport and Tourism, 2020). Therefore, there has been a strong need to manage forests for sustainable water supply from mountains even under drought conditions (Forestry Agency, 2019).

Forest thinning is among the most effective silvicultural treatments of forest management to increase water availability for humans (Ganatsios et al., 2010; Hawthorne et al., 2013; Sun et al., 2015a). The forest thinning effects on the catchment hydrology would be primarily due to changes in evapotranspiration (ET), induced by alterations to the forest canopy-atmosphere processes (Komatsu et al., 2007; Sun et al., 2014). Numerous studies have been conducted on the thinning effect on ET in coniferous plantations in Japan. They found that thinning

* Corresponding author at: Department of Forest Science, Graduate School of Agricultural and Life Sciences, The University of Tokyo, 1-1-1 Yayoi, Bunkyo-ku, Tokyo 113-8657, Japan.

E-mail address: momiyama@g.ecc.u-tokyo.ac.jp (H. Momiyama).

<https://doi.org/10.1016/j.foreco.2021.119593>

Received 16 April 2021; Received in revised form 30 July 2021; Accepted 3 August 2021

0378-1127/© 2021 Elsevier B.V. All rights reserved.

decreases transpiration (T_r ; Komatsu et al., 2013; Morikawa et al. 1986; Sun et al., 2014; Tateishi et al., 2015) and increases floor evaporation (E_f ; Sun et al., 2016). Using a model, Komatsu (2020) also estimated that $T_r + E_f$ becomes almost the same before and after thinning. On the other hand, interception (I_c) is related to the stem density (S_d) of the plot (Komatsu et al., 2007), and most of the previous studies show a reduction in I_c due to thinning (Hattori & Chikaarashi, 1988; Nanko et al., 2016; Shinohara et al., 2015; Sun et al., 2015b) with the exception (Kubota et al., 2018). However, despite the findings of the thinning effect on ET, these findings have not been reflected in analyses using rainfall-runoff models. Although many long-term observations are also necessary when considering the interannual variability of thinning impacts, the number of sites which the long-term effects of thinning have been observed are insufficient (Liu et al., 2018; Komatsu, 2020). Moreover, as runoff is originated from net precipitation input to the catchment water storage, soil physics related to the water holding capacity and conductivity can supplementarily alter the thinning effects on the water availability (Moreno et al., 2016; Zhang et al., 2016). Here, we emphasize that to quantify the hydrological effect of forest thinning, we should take into consideration the combined effects of the ET change and the soil physics properties on the runoff from the studied catchment.

There have been numerous findings of the relationships between forest cover change and runoff responses based on observational and experimental studies (Bosch & Hewlett, 1982; Brown et al., 2005). However, generalizing these findings and predicting the water yield after forest thinning in either catchment by observations alone have been difficult because of varieties of climate, vegetation type, geology, and topography (McDonnell et al., 2018; Saksu et al., 2017). What is less certain is the forest thinning effects on increasing both minimum seasonal streamflow rate during the drought periods of the year and extremely low streamflow rate during the prolonged drought periods (see Smakhtin, 2001). Note that it should be also difficult to obtain so sufficient long-term climate data that can explain the influence of an extraordinary drought on the thinning effects.

Our goal is to investigate how forest thinning affects water yield from a headwater catchment, especially under abnormally severe and common drought conditions. Toward this goal, we use 100-year meteorological data generated by observed precipitation statistics, a semi-process-based rainfall-runoff model (a modified TOPMODEL; cf. Beven & Kirkby, 1979), and detailed catchment-hydrology observations conducted over an 8-year period. Prior to accessing the thinning impacts in terms of low-flow hydrology, the model is first validated with the field observations at a forested mountain catchment in the Kanto region of Japan, described next.

2. Study site and observations

2.1. Site description

This study was carried out in the Oborasawa Experimental Watershed (OEW), a 55-ha forest headwater catchment in the Tanzawa mountains, in the Kanto region of Japan (Fig. 1; Table 1). The catchment is steep with a mean slope (\pm standard deviation [SD]) of $34.9 \pm 9.0^\circ$. The soil is classified as Cambisol having a large portion of volcanic ash and has a high infiltration capacity at the surface ranging from 100 to 600 mm h⁻¹ (Oda et al., 2013). The mean soil depth (\pm SD), observed by a cone penetration test, was 1.64 ± 0.97 m ($n = 217$; Yokoyama et al., 2014). The underlying bedrock beneath the soil is tuff, composed mainly of volcanic breccia, and is classified as Cenozoic sedimentary rock. There exists weathered bedrock with fissures below 40 m depth from the surface, and its hydraulic conductivities depend on the degree of weathering, ranging from 4.7×10^{-5} to 2.6×10^{-6} cm s⁻¹ (Yokoyama et al., 2013).

The mean annual precipitation (P) for the period 2010–2017 was 2954 mm. Large rainfall events occur generally during the rainy season from mid-June to early July (584 ± 206 mm for the 2-month June–July;

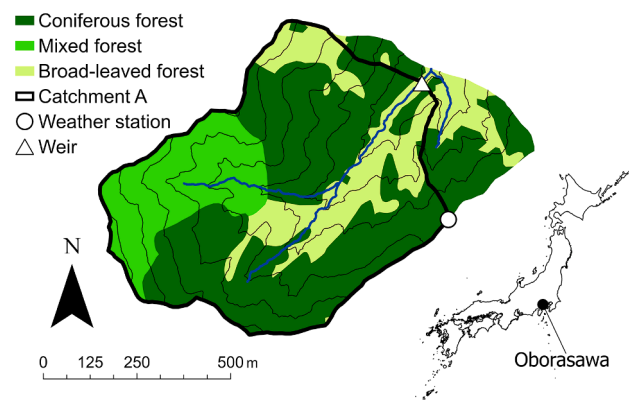


Fig. 1. Location, topography, and vegetation of Oborasawa watershed. The contour line intervals are 50 m.

Table 1
Characteristics of Oborasawa.

Location	35°28'N, 139°12'E
Catchment area	49.5 ha (Catchment A)
Altitude	439–872 m
Mean annual rainfall	2954 mm
Mean air temperature	11.6 °C
Stem density	1280 trees ha ⁻¹
LAI	3.8 m ² m ⁻²

mean \pm SD) and the typhoon season from September to October (921 ± 235 mm). Snowfall only occurs once or twice a year from January to March, only accounts for a small percentage of total annual precipitation, and has limited influence on runoff. The annual mean air temperature (T_a) was 11.6 °C between 2010 and 2017, with an annual minimum daily mean T_a of -2.5 °C around January and an annual maximum daily mean of T_a of 24.4 °C around August. The mean daily vapor pressure deficit (VPD) averaged over daylight hours (06:00–18:00 LT) reached a maximum of 1.6 kPa in May.

Forest in the OEW consists mainly of coniferous plantation stands, and the bare land ratio is less than 1%. Approximately two-thirds of the forested areas are composed of conifers, i.e., *Cryptomeria japonica* D. Don and to a lesser extent, *Chamaecyparis obtusa* Endl. (a vegetation survey in 2007; Uchiyama et al., 2014). The remaining one-third is fragmented areas of deciduous broadleaved trees, e.g., *Cercidiphyllum japonicum* Sieb. et Zucc. and *Aesculus turbinata* Blume. The averaged S_d and leaf area index (LAI) over the catchment were estimated to be 1280 trees ha⁻¹ and 3.8 m² m⁻², respectively.

2.2. Hydrological and micrometeorological observations

A 49-ha subcatchment (referred to as Catchment A) of the OEW is devoted to catchment-scale water budget observations. A previous study using the annual chloride balance method (Oda et al., 2013) assumed little bedrock drainage and inter-catchment groundwater flow, which was ca. 5% of annual runoff and almost negligible, in Catchment A, although the recently accumulated observation data suggest that the bedrock drainage and/or spring could be larger than the previous estimation (data not shown here).

The data from the 2010–2017 observations were used for this study. The stream water level was measured every 10-min by a pressure type water level gauge (ATM_N type, Koshin Denki, Tokyo, Japan) installed at a V-notch weir in Catchment A, and was converted to volumetric runoff (Q_v) with an empirical relationship between the water level and actual Q_v . Then, specific discharge, hereinafter referred to as runoff (Q), was obtained by dividing Q_v by contributing catchment area. The P was continuously measured every 10-min with a 0.5 mm tipping-bucket rain

gauge (N78, Nippon Electric Instrument, Tokyo, Japan) at the open ridge in Catchment A (Fig. 1).

Solar radiation (R_s) and relative humidity (RH) and T_a were measured every 10-min at the open ridge of Catchment A using a pyranometer (SL-30, Azbil, Tokyo, Japan) and a relative humidity probe (HT-20, Azbil, Tokyo, Japan), respectively. The VPD was calculated as a saturated vapor pressure of T_a minus an actual vapor pressure estimated from RH, and then, was averaged over daylight hours (06:00–18:00 LT).

3. Methodology

We discuss first the rainfall-runoff model development, validating the model, and parameterization, and then proceed to discuss its usage for assessing the forest thinning effect on runoff regimes under normal and abnormal drought conditions following the precipitation statistics. For the model validation, the observed meteorological variables time series were used to drive the model calculation; however, in our model simulations for the severe drought impact—only precipitation statistics were available thereby necessitating a stochastic representation such as the flow duration curve (cf. Yokoo & Sivapalan, 2011). The generation of 100-year meteorological data and the connections to the flow duration outputs are also discussed.

3.1. Rainfall-Runoff model

Given little bedrock drainage and inter-catchment groundwater flow, the Q can be expressed as the function of soil water storage, following the original TOPMODEL concept (Beven & Kirkby, 1979). In this study, TOPMODEL was modified to account for the forest thinning impact on ET and the resultant Q . Note that according to our preliminary approximate estimate of the time lag between P and Q at a daily time scale in the study catchment, we did not take into consideration water storage capacity in the root or vadose zone (e.g., Beven et al., 1995) for this modification.

The vertically integrated continuity equation describes the catchment water balance (Fig. 2) to compute the catchment average saturation deficit \bar{D}_s (mm), given by

$$\frac{d\bar{D}_s}{dt} = T_r + I_c + Q_{\text{over}} + Q_{\text{sub}} - P, \quad (1)$$

where t is time (day), Q_{over} is overland flow (mm day^{-1}), and Q_{sub} is subsurface flow (mm day^{-1}). Saturation deficit at a given point i ($D_{s,i}$; mm) can be calculated as:

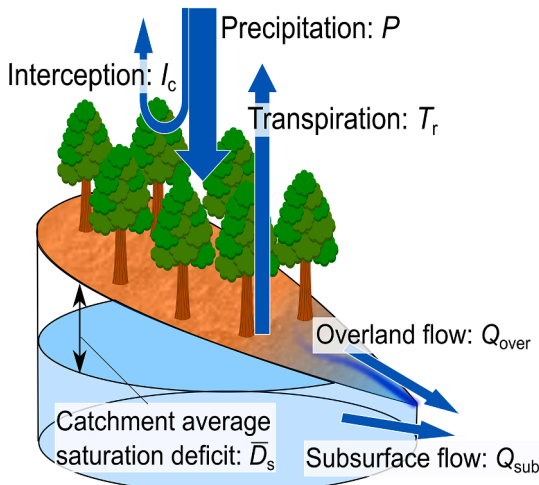


Fig. 2. Schematic diagram of the rainfall-runoff model used in this study.

$$D_{s,i} = \bar{D}_s + m(\bar{\text{TI}} - \text{TI}_i), \quad (2)$$

where m is a soil parameter replacing ϕ/f , in which ϕ is soil porosity and f defines the decrease of saturated hydraulic conductivity with depth, and $\bar{\text{TI}}$ and TI_i are the topographic indices TI as the catchment average and the value at a given point i , respectively. TI is defined as $\ln(a/\tan\beta)$, in which a is contributing catchment area per unit contour length and β is the local slope. For the TI computation in this study, using a 1-m gridded digital elevation model (DEM), all pits were made level with theoretically elevation increments (Ao et al., 2003) and the multiple flow direction algorithm was adopted (Quinn et al., 1991).

Q_{over} and Q_{sub} in Eq. (1) are respectively given by

$$Q_{\text{over}} = \frac{1}{N} \sum_{i=1}^N \max(0, -k_i D_{s,i}) \quad (3)$$

and

$$Q_{\text{sub}} = T_{\text{max}} e^{-\bar{\text{TI}}} e^{-\frac{\bar{D}_s}{m}}, \quad (4)$$

where N is the number of grids in the DEM of the studied catchment, k_i is a time constant, and T_{max} is a soil parameter representing the transmissivity, which replaces K_0/f , in which K_0 is the saturated hydraulic conductivity at the surface.

3.2. Evapotranspiration modeling

The ET model, incorporated into the rainfall-runoff model in this study, comprises T_r and I_c models based on the formulations by Momiyama et al. (2019). In general, the boundary conductance of conifers is sufficiently large, and Kumagai et al. (2008) confirmed *Cr. japonica* canopies are aerodynamically well coupled to the atmosphere. Hence, we used a modified McNaughton and Black (1973) expression to compute the daily T_r rate given by

$$T_r = 12 \times 3600 \times \alpha \frac{\rho_a c_p \text{VPD}}{\rho_w \lambda \gamma} G_s, \quad (5)$$

where α is a limiting parameter for T_r , ρ_a is the density of dry air (kg m^{-3}), c_p is the heat capacity of air ($\text{J kg}^{-1} \text{K}^{-1}$), ρ_w is the density of water (kg m^{-3}), λ is the latent heat of vaporization of water (J kg^{-1}), and γ is a psychrometric constant (Pa K^{-1}). The G_s is the monthly mean surface conductance (mm s^{-1}), which was calculated from the inverse form of Eq. (5) with the monthly mean T_r . Note that the T_r was calculated by subtracting the estimated I_c (described later) from the monthly mean ET derived from the short-term water budget method at the studied catchment (cf. Momiyama et al., 2019). Here, given the daily estimation in the mid-latitude zone, the T_r rate per second was summed over daylight hours ($=12 \text{ h} \times 3600 \text{ s}$) with mean daytime VPD (Pa).

Major uncertainties for driving Eq. (5) are G_s and α which are generally functions of environmental variables, e.g., R_s (W m^{-2}) and VPD in kPa for G_s and soil moisture for α . Here, the monthly mean G_s in the studied catchment is expressed using a multiplicative-type function (e.g., Jarvis, 1976):

$$G_s = 4.30 \times 10^{-3} \bar{R}_s \times (1 - 5.78 \times \ln \bar{\text{VPD}}), \quad (6)$$

where an overbar denotes a monthly mean value. According to Tadaki's (1976) report, in Japan, LAI of common coniferous plantations can be estimated to be at least >3.0 , and foliage amount per ground area in forests with closed canopy is independent of the forest thinning intensity and the stand density. Thus, we assumed that the G_s is conservative against changing LAI at post-thinning (cf. Kelliher et al., 1995). To facilitate the interpretation of the influence of drought conditions on T_r and the resultant Q , we assumed the following:

$$\alpha = \begin{cases} 0, & \text{for } \overline{D_s} > D_{sx}, \\ 1, & \text{for } \overline{D_s} \leq D_{sx}, \end{cases} \quad (7)$$

where D_{sx} is $\overline{D_s}$ at plant wilting point. That is, α abruptly decreases to zero under severe drought conditions and has unity for wet conditions.

Komatsu et al. (2007) found a moderate relationship between the I_c ratio, which represents the I_c loss divided by annual P , and the S_d from 12 previous studies throughout Japan ($R^2 = 0.42$), leading to

$$I_c = P \times (4.98 \times 10^{-5} S_d + 0.12) \quad (8)$$

Kumagai et al. (2014) suggested that Eq. (8) might be applicable to estimates at a more detailed time scale, and thus we assumed that the daily I_c loss can be estimated using Eq. (8) with daily P . It should be noted that the estimated I_c ratio in Eq. (8) ($=0.184$, in which $S_d = 1280$ trees ha^{-1}) for the studied catchment is consistent with the preliminary observations at the several sites in the OEW (0.14–0.25).

3.3. Model calibration

To estimate model parameters, i.e., m , T_{max} , D_{sx} , and $\overline{D_{s0}}$ (an initial value of $\overline{D_s}$), Q in the modified TOPMODEL was calibrated by comparing the simulated Q with the 8-year observation through the shuffled complex evolution (SCE-UA) algorithm (Duan et al., 1993, 1992). Given the importance of low streamflow in this study, we used Nash–Sutcliffe efficiency (Nash & Sutcliffe, 1970) criterion with inverse Q values (NSE_{inv}) as an evaluation function for the optimization (Pushpalatha et al., 2012), given by

$$NSE_{inv} = 1 - \frac{\sum_{j=1}^n \left(\frac{1}{Q_{oj}} - \frac{1}{Q_{mj}} \right)^2}{\sum_{j=1}^n \left(\frac{1}{Q_{oj}} - \overline{\left(\frac{1}{Q_{oj}} \right)} \right)^2}, \quad (9)$$

where n is the total number of time steps, subscript j denotes each time step, Q_o and Q_m are observed and simulated Q , respectively, and overbar denotes ensemble mean.

We performed four types of calibrations to examine which model parameters dominate the model reproducibility for observations (see Table 2). Case A optimizes all four parameters, i.e., m , T_{max} , D_{sx} , and $\overline{D_{s0}}$, taking into consideration groundwater runoff, Q_{sub} , and soil moisture limitation for T_r . Cases B and C assume not accounting for Q_{sub} ($T_{max} = 0$) and the soil moisture limitation ($D_{sx} \rightarrow \infty$), respectively, and optimize remaining parameters, i.e., m , D_{sx} , and $\overline{D_{s0}}$ for Case B and m , T_{max} , and $\overline{D_{s0}}$ for Case C. Case D takes into consideration neither Q_{sub} nor the soil moisture limitation, optimizing only two parameters, m and $\overline{D_{s0}}$.

3.4. Numerical experiments

Numerical experiments examining the hydrological impacts of forest thinning were based on changing the variable S_d in Eq. (8) in this study. For simulation purposes, meteorological data in the period of 100-year with 2-year for spin-up were constructed using random numbers generated from probability distributions representing current P characteristics at the site. The current P characteristics were taken from 8-

Table 2
Calibrated model parameters and Nash–Sutcliffe efficiency criterion with inverse runoff values (NSE_{inv}) for each Case.

Cases	m (m)	T_{max} ($m^2 h^{-1}$)	D_{sx} (m)	$\overline{D_{s0}}$ (m)	NSE_{inv}
A	0.0493	0.0628	0.222	0.247	0.827
B	0.0445	NA	0.177	0.203	0.827
C	0.0520	0.00248 ^a	NA	0.236	0.749
D	0.0517	NA	NA	0.233	0.749

^a Parameterized at the detection limit.

year P records collected in 2010–2017. As a result of the rainfall-runoff model simulations with the 100-year meteorological data, 100-year time series of Q (and additionally, the other hydrological components, e.g., ET) can be computed. From the simulated time series of Q , flow duration curves for the 100-year and the low-flow domain in each year can then be obtained. Shifts in the low-flow rate of each year within the 100-year can then be readily related to thinning intensities and soil physics.

The P time series were constructed as follows: in each month, the frequency of rainfall events was determined by the Markov chain method (cf. Gabriel & Neumann, 1962), and then, the amount of rainfall when rainfall occurs was assumed to be an independent random variable, expressed by a mixed exponential distribution (cf. Wilks & Wilby, 1999). It is logical to anticipate that P changes lead to concurrent changes in other meteorological variables such as VPD and R_s because of increased or decreased atmospheric moisture content and cloud cover. Here, the daily mean VPD values related to daily P were obtained as random numbers generated by Weibull distributions representing the probability density functions of the VPD in five bin ranges of the P . Also, the daily mean R_s related to the VPD were obtained in the same manner as for the VPD but using Weibull distributions of the R_s in five bins of the VPD for each month.

For the analysis, ‘Intermediate Flows’ and ‘Low flows’ were defined to consider the effect of thinning on drought period during the year. ‘Normal Years’ and ‘Dry Years’ were defined to consider years with particularly low ‘Low Flow’. These were determined as follows: In each flow duration curve of the 100-year simulation, the flows within the ranges of 20–70% and >70% time exceedance were referred to as ‘Intermediate flows’ and ‘Low flows’, respectively (cf. Yilmaz et al., 2008). Besides, the simulation years when the averaged flows in the ‘Low flows’ domain of the simulated flow duration curves for Case B and $S_d = 1280$ trees ha^{-1} are the lowest and 50th the lowest were referred to as ‘Dry year’ and ‘Normal year’, respectively. We investigate the shifts in flows of Intermediate flows and Low flows corresponding to changes in S_d and/or soil physics under Normal year and Dry year conditions.

4. Results

4.1. Validation of the rainfall-runoff model

At a yearly time scale, we estimated ET by catchment water balance between P and Q and divided the ET into T_r and I_c by subtracting the I_c estimated using Eq. (8) from the ET (Fig. 3). Given little bedrock drainage in the studied catchment and the Q expressed as the function of catchment water storage, a previous study (Momiya et al., 2019) estimated monthly mean daily ET over the 8-year observation campaign using the short-term water budget method (see Linsley et al., 1958; Suzuki, 1985) (Fig. 4).

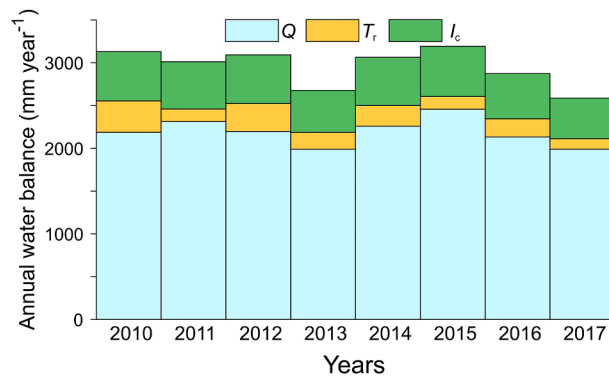


Fig. 3. Annual water balance in the studied catchment. Q , T_r , and I_c denote runoff, transpiration, and interception, respectively, and the sums of them are precipitation.

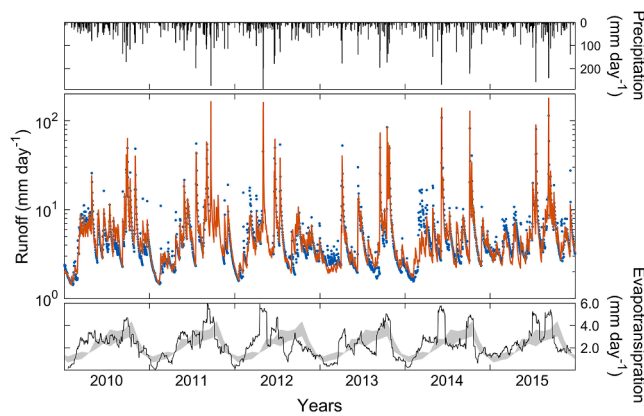


Fig. 4. Precipitation (upper panel), observed (closed circles) and modeled (solid line) runoff (middle panel), and observed (grey zone, representing the range of middle quartiles of the data) and modeled (solid line) evapotranspiration (lower panel) in the studied catchment. The model simulation was conducted using the parameter set in Case B (see Table 2). The observed daily evapotranspiration rates were obtained as monthly-mean values in an averaged single annual variation in the period 2010–2017, estimated by the short-term water budget method. Note that the single annual variation repeatedly appears every year. Daily-computed evapotranspiration rates were converted to 31-day moving average values, resulting in the modeled daily evapotranspiration rates.

As a result of comparisons among NSE_{inv} for Cases A–D, we found that NSE_{inv} for Cases A and B are almost the same (0.827) and the highest, suggesting that Case B, which neglects the effect of Q_{sub} on Q , i.e., the parameter T_{max} , performed the best (Table 2). Also, NSE_{inv} for Cases C and D are almost the same (0.749) and still an acceptable value for the reproduction of the data, although the value is less than that for Case B. This suggests that for the simulation of water balance in this studied catchment using this rainfall-runoff model, a model parameter calibration of the only m is sufficient, and adding another model calibration of D_{sx} contributes to the reproduction skill of this model. Thus, hereinafter we use Cases B and D for the model investigations.

Daily variations in calculated Q and ET with the parameter set in Case B (see Table 2), forced by observed meteorological variables, are compared against observations for January 1, 2010, to December 31, 2015, in Fig. 4. The model well reproduced observed Q and ET despite all the simplifying assumptions. Fig. 5 further compares simulated flow duration curves, which were made of calculated Q forced by the 8-year observed and the 100-year generated meteorological data with the

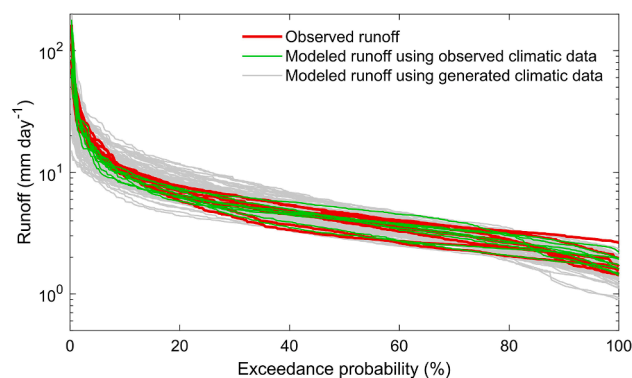


Fig. 5. Flow duration curves made of observed runoff in 2010–2017 (red lines) and modeled runoff using observed climatic data in 2010–2017 (green lines) and generated climatic data for 100-year (grey lines). The model simulations were conducted using the parameter set in Case B (see Table 2). (For interpretation of the references to color in this figure legend, the reader is referred to the web version of this article.)

parameter set in Case B (see Table 2), against flow duration curves made of the 8-year observed Q . In terms of averaged Q over the Low flow domain (Q_{LF}) and the Intermediate flow domain (Q_{IF}) in Fig. 5, there were no significant differences between both mean and variance of the 8-year observed Q_{LF} and those of the 8-year ($p = 0.93$, t -test; $p = 0.49$, F -test) and the 100-year ($p = 0.61$, t -test; $p = 0.52$, F -test) modeled Q_{LF} , and between those of the 8-year observed Q_{IF} and those of the 8-year ($p = 0.84$, t -test; $p = 0.87$, F -test) and the 100-year ($p = 0.36$, t -test; $p = 0.50$, F -test) modeled Q_{IF} . This confirms the successful reproduction of the stochastic characteristics of both actual Q_{LF} and Q_{IF} using the 100-year generated meteorological variables.

4.2. Thinning impacts on runoff

Fig. 6 shows simulation results on relationships between S_d and Q and ET using the 100-year generated meteorological data and Cases B and D parameter sets (see Table 2). A decrease in S_d increased Q owing to a reduction in ET , despite the small thinning effects on increases in Q_{LF} , in both Normal year and Dry year. In general, with decreases in S_d , increasing ratios of Q were lower than decreasing ratios of ET , and this tendency became more pronounced for Q_{LF} . Also, comparing simulation results of Cases B and D, the soil water deficit control on T_r (see Eq. (7)) was found to contribute to enhancing Q_{LF} more appreciably than Q_{IF} in Normal and Dry years (Fig. 6).

Before the investigation on the forest thinning impacts via alterations of ET and soil physics properties, we evaluate a single hydrological effect of the catchment soil physics (here, referred to as catchment water retention capacity, m in Eq. (2)) on Q with changing the parameter m in Case D (Fig. 7). While simulated Q was relatively robust to an increase in m , the smaller m compared to the reference value (0.0517 m; see Table 2), i.e., the smaller catchment water retention capacity, significantly reduced Q_{LF} . Fig. 8 compares the simulation results of relationships between m and increases in Q_{LF} and Q_{IF} due to the thinning in Normal and Dry years. Two thinning scenarios are presented: one is from 1500 ha^{-1} to 1000 ha^{-1} with reference to the estimated S_d of the study site (1280 trees ha^{-1} ; Fig. 8a, c), and the other assumes intense thinning, from 2229 ha^{-1} to 1132 ha^{-1} , based on Kubota et al. (2018) (Fig. 8b, d). There was somewhat exponential saturation in the relationships: high values of increases in Q_{LF} and Q_{IF} in higher m (>0.0517 m), and drastically decreases in the values with m decreasing (Fig. 8). Again, the hydrological effects of the forest thinning on increasing water resources were confirmed to be very small under severe drought conditions. It is interesting to note that unlike the other cases, the runoff growth rate (i.e., the ratio of runoff after to before thinning) for Q_{LF} in the Dry year decreased and became constant with increasing m (Fig. 8c, d). This is because a majority of Q_{LF} might be derived from catchment stored water and hence intrinsic Q_{LF} before thinning, especially in the Dry year, tends to decrease with decreasing m .

5. Discussion and conclusion

5.1. Validating the model

Forest thinning will firstly increase net precipitation (P_{net}) into the surface soil layer via a reduction in I_c , and then increase Q with changing consumption of the surface water storage by the T_r and E_f . Thus, we assume how to describe the thinning impact on ET , i.e., $I_c + T_r + E_f$ is the most critical in modeling total water balance amenable to forest thinning.

Komatsu (2020) asserted that forest thinning significantly affects I_c and least changes $T_r + E_f$. Also, he suggested that in terms of the robust $T_r + E_f$, some cancellations emerge; an intense thinning decreases stand-scale T_r but increases E_f with increasing canopy openness and incident radiative energy to the forest floor. While, some previous studies (e.g., Gebhardt et al., 2014; Sun et al., 2014) reported an increase in individual-scale T_r after thinning probably because of relaxing

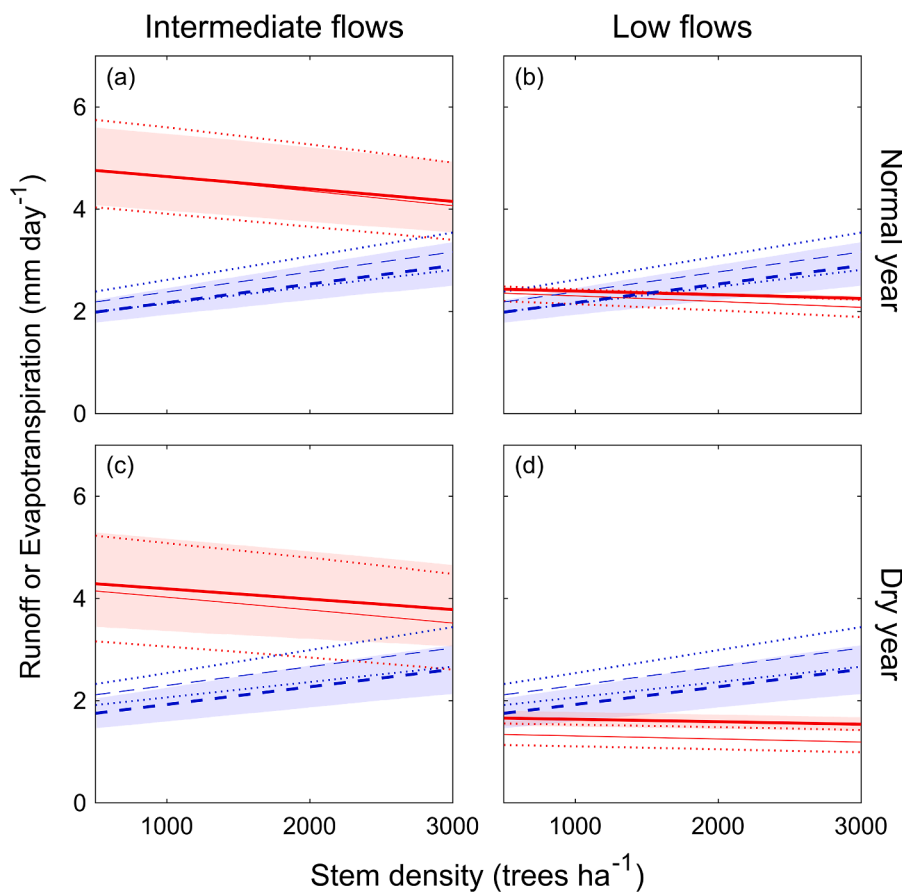


Fig. 6. Modeled relationships between stem density and runoff (red solid lines) and evapotranspiration (blue broken lines) using 100-year generated climatic data. Both thick lines with shaded zone and thin lines with ranges between upper and lower dotted lines represent averages with the upper 10–90% values, modeled with (Case B) and without (Case D) taking into consideration the effect of soil water deficit on transpiration, respectively (see Table 2). Columns (a, c) and (b, d) are model results for Intermediate flows and Low flows situations, respectively, and rows (a, b) and (c, d) are ones for the Normal year and the Dry year, respectively. (For interpretation of the references to color in this figure legend, the reader is referred to the web version of this article.)

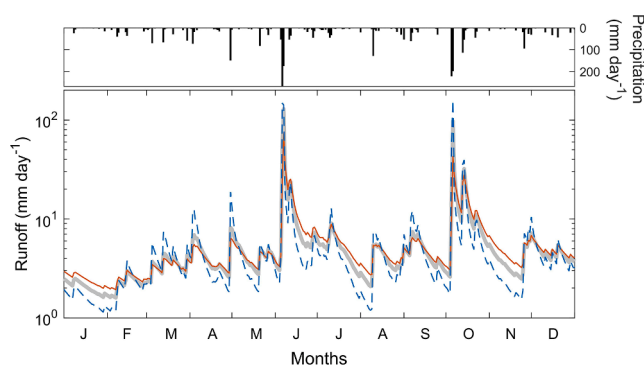


Fig. 7. Daily precipitation (upper panel), and modeled daily runoff (lower panel) using $m = 0.0517$ (thick solid line), $m = 0.07$ (thin solid line) and $m = 0.03$ (thin broken line) in the studied catchment in 2014. The model simulations were conducted changing the only m in parameters in Case D (see Table 2).

remaining trees from resource competitions, which might result in the little change in stand-scale T_r . In this study, according to Kelliher et al. (1995), we formulated the stand-scale T_r characteristics, i.e., the G_s (Eq. (6)), to be conservative against LAI or S_d after thinning. Although how the T_r characteristics are altered by thinning has been still unclear, our assumption on the conservative G_s would be equivalent to Komatsu's (2020) assertion on the conservative $T_r + E_f$. In Japan, most coniferous plantations are evergreen forests, and the proportion of R_s that reaches the forest floor is not expected to change with season (Sun et al., 2016). A previous study also showed that the seasonal variation in E_f did not vary significantly with T_r (Sun et al., 2017). Therefore, if $T_r + E_f$ is constant, the proportion of E_f will not significantly affect the simulation

results. Note that while thinning coniferous plantations in Japan results in a decrease in stand-scale T_r (Komatsu et al., 2013; Morikawa et al. 1986; Sun et al., 2014; Tateishi et al., 2015), very few studies have examined long-term changes in ET (Komatsu, 2020). To examine this assumption, further observation of long-term changes in ET is necessary.

As a result, a submodel describing the thinning impact on I_c can be assumed to control a majority of the simulated ET under forest thinning conditions. To estimate daily values of I_c , we employed the I_c model (Eq. (8)) which was originally developed by Komatsu et al. (2007). In reality, although the I_c ratio in Eq. (8) on the present S_d condition for the study catchment was within a range of preliminary short-term observations at multiple plots, it overestimated the measured value at our single long-term intensive ET observation plot in the same catchment (see Fujime et al., 2021). On the other hand, Shinohara et al. (2015) reported that immediately after thinning at their site in Japan, I_c decreased to a greater extent than the estimations by Eq. (8). These could lead to the underestimation of an increase in P_{net} due to thinning. Despite successful reproduction of the actual Q by using the estimated P_{net} and tuning soil physics parameters in the present model, the appropriate estimation of the catchment-scale I_c altered by forest thinning remains controversial and requires more technically difficult examinations.

Although our method enables ET estimation from observations of runoff and meteorological factors, there is still some uncertainty in this method. We estimated ET from the catchment water balance. This is based on little bedrock drainage and inter-catchment groundwater flow at OEW (Oda et al., 2013). Snowfall and snowmelt may affect ET estimation (Momiyama et al., 2019). T_r estimated from the short-term water budget method reproduced observed T_r at a plot in OEW by the thermal dissipation method, except for winter and early spring (Fujime et al., 2021). The uncertainty of the estimation of I_c mentioned above can also affect the estimation of T_r because T_r is estimated by $ET - I_c$ (Fig. 3), and the overestimated I_c may lead to the underestimation of T_r .

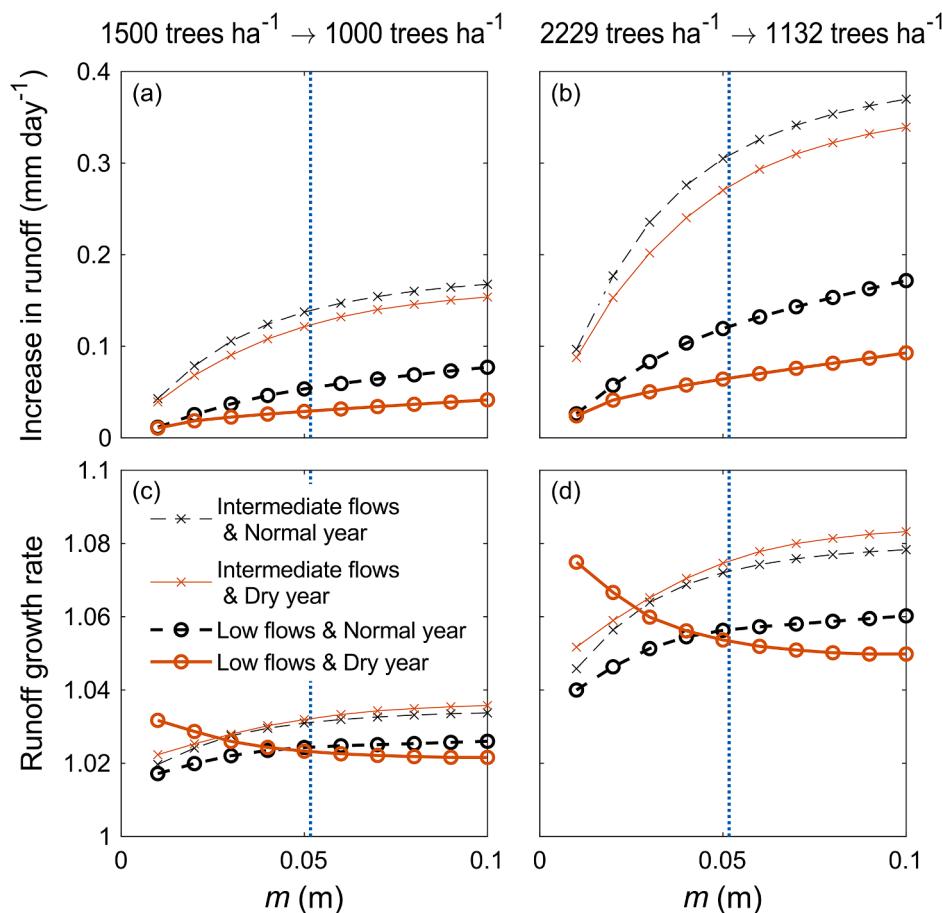


Fig. 8. Relationships between the parameter m and increases in runoff (a, b) and runoff growth rate (c, d) after thinning. The model simulations were conducted changing the only m in parameters in Case D (see Table 2). Columns (a, c) and (b, d) represent changes in the values due to alterations of stand density, 1500 to 1000 trees ha^{-1} and 2229 to 1132 trees ha^{-1} , respectively. The relationships are compared between Intermediate flows and Low flows situations and between the Normal year and the Dry year. Vertical dotted lines denote the m estimated for the actual data (0.0517 m).

As a result of optimization, the model considering $T_{\max} = 0$ performed as well as the model considering the optimized T_{\max} (Table 2). When considering $T_{\max} = 0$ in the TOPMODEL (see Eqs. (3) and (4)) used to reproduce the total runoff (Q) from the studied catchment, a lumped rainfall-runoff model, the so-called tank model (Sugawara, 1972, 1995), can be compatible with the TOPMODEL. Neglecting detailed information on soil moisture dynamics distributed over the catchment, multiple discharges (q_i) from a single tank were assumed as:

$$Q = \sum_{i=1}^N q_i = \sum_{i=1}^N \max\{0, a_i(H - h_i)\}, \quad (10)$$

where N is the number of discharge holes of the tank, i identifies each discharge hole, a_i and h_i are fitting parameters, and H is the current depth of water in the tank. Note that h_i represents the height of the discharge hole i from the bottom of the tank. A comparison between Eqs. (3) and (10) allows us to derive the following relationships:

$$a_i = \frac{k_i}{N}, \quad (11)$$

$$H = -\bar{D}_s + C, \quad (12)$$

and

$$h_i = m(\bar{\text{TI}} - \text{TI}_i) + C, \quad (13)$$

where C is a constant to make H and h_i positive, and a_i is found to be a constant independent of i . Further, we confirmed that the soil parameter m in the TOPMODEL denotes catchment water retention capacity because an increase in h_i delays the start of discharge from the stored water in the tank, and h_i can be linearly related to m in Eq. (13). Indeed, a decrease in m reduced the calculated Q_{LF} , i.e., baseflow through the

increasing flood following precipitation (Fig. 7). Again, at least in this studied catchment, tuning only one soil physics parameter m can provide sufficient reproducibility of actual Q (Table 2). This suggests that catchment water storage is a major driver of the Q from the studied catchment. As only this parameter explains the water retention capacity in this model, m may include the effect of bedrock (Kosugi et al., 2006) or vertical unsaturated flow (Tani et al., 2020). Although m in the modified TOPMODEL may be different from that intended in the original TOPMODEL, the change in soil physics can also be explained by m , and we can possibly consider the hydrological effect of catchment water retention capacity when the degree to which m would be altered by thinning is known.

Despite few historical records on the Q impacted by forest thinning treatments, several previous studies demonstrated that in the temperate zone, percentages of annual Q increase to annual P due to thinning (ΔQ : %) ranged from 1.3 to 6.2% and from 2.0 to 15% when ca. 30 and 50% of the stems in the catchments were removed, respectively (Baker, 1986; Bosch & Hewlett, 1982; Bren et al., 2010; Hawthorne et al. 2013; Jayasuriya et al., 1993; Lesch & Scott, 1997). In Japan, Kubota et al. (2018) reported that a 3-year mean ΔQ after thinning from 2229 to 1132 trees ha^{-1} , which is identical to ca. 50% thinning, was 3.2% at the Ch. obtusa catchment. The simulations by our rainfall-runoff model, that is, the modified TOPMODEL in this study, estimated ΔQ after thinning from 2229 to 1132 trees ha^{-1} and from 1500 to 1000 trees ha^{-1} (ca. 30% thinning) to be 5.2 and 2.4%, respectively (cf. Figs. 6 and 8), falling within the range of actual records. Thus, we assumed that the rainfall-runoff model would have a sufficient ability to examine the forest thinning impacts on water resources in forested catchments.

Note that the I_c modeling can be assumed the most important for the simulations to examine the thinning impact on ET (Komatsu, 2020). Here, we adopted the I_c model with the best performance for changing

S_d , i.e., thinning intensities (Komatsu et al., 2007). In other words, the I_c model would allow us to best simulate P_{net} corresponding to a large variety of thinning intensity. Furthermore, our rainfall-runoff model well reproduced the 8-year Q observation, in particular, the Q_{LF} record (see Fig. 5). This ensures that the model can successfully simulate Q , especially Q_{IF} and Q_{LF} , with the changing P_{net} input to the catchment surface. Therefore, using this model simulation, we can expect a highly reliable prediction of Q_{IF} and Q_{LF} regimes affected by forest thinning, discussed next.

5.2. Analyzing the model simulations

Many previous studies on how water supply from forested headwaters will increase through a decrease in the forest water use due to forest harvesting have been performed using empirical and experimental methods (see McDonnell et al., 2018). In Japan, both policymakers and people have anticipated conservation and optimization of water resources from forested headwaters by appropriate forest management, mainly expecting to maintain the water supply in a shortage of precipitation, i.e., Q_{LF} and further, one in the Dry year. However, without sufficient scientific evidence, the policy recommendations about forest thinning for increasing available mountain water resources have been claimed (cf. Fujimori, 2006). In our present study, the rainfall-runoff model was validated by previous observational studies, and stochastic treatments for P regimes enabled us to examine the thinning impacts on hydrological processes under Low flows conditions in both Normal and Dry years (see Kumagai et al., 2004; Yokoo & Sivapalan, 2011). For example, the simulated increases in Q_{LF} and Q_{IF} due to thinning from 3000 to 1000 trees ha^{-1} (hereinafter, referred to as ΔQ_{LF} and ΔQ_{IF} , respectively) without the T_r regulation were 0.22 and 0.57 $mm\ day^{-1}$, respectively in the Normal year and 0.12 and 0.50 $mm\ day^{-1}$, in the Dry year (Fig. 6). This revealed that the policy recommendations have been exaggerated, especially concerning Low flows and Dry year conditions.

The D_{sx} obtained for Cases A and B (Table 2) mean sensitive water use regulation against small \bar{D}_s in the studied forest catchment composed of *Cr. japonica*, *Ch. obtusa*, and various hardwood species. On the other hand, Kumagai et al. (2008) indicate that *Cr. japonica* tends to have little regulation of tree water use even during the sporadic periods of severe soil drying, expecting $D_{sx} \rightarrow \infty$ (see Table 2) for a single *Cr. japonica* species stand. Then, it is instructive to consider the forest manipulation effects on hydrology from the supposition that changing forest stand status from 3000 trees ha^{-1} without the T_r regulation to 1000 trees ha^{-1} with the T_r regulation denotes a forest thinning with changing the species composition such as from a single *Cr. japonica* species stand as “a heavy drinker” to a multi-species stand like the studied catchment as “a miser”.

Given this forest manipulation, ΔQ_{LF} and ΔQ_{IF} were 0.32 and 0.57 $mm\ day^{-1}$, respectively in the Normal year and 0.45 and 0.67 $mm\ day^{-1}$, in the Dry year (Fig. 6). The base parameters set was obtained assuming a multi-species stand, i.e., actually studied catchment, as Case B, while the parameters set of Case D assumes a single *Cr. japonica* stand, which is a very common forest stand type in Japan. Here we have to note that the m optimized for Case D adjusts Q without water use regulation by trees, and therefore is larger than the one for Case B (Table 2). Hence, based on the Case B parameter set, which was determined for actual Q data, Q_{LF} and Q_{IF} without the water use regulation and with the same m as Case B would be smaller than those in Case D, implying that the estimated ΔQ_{LF} and ΔQ_{IF} could be minimum predicted values. This suggests that the forest thinning with the conversion of the species might be promising forest management for sustainable mountain water resources, especially under severe precipitation shortage conditions.

The review study by Smakhtin (2001) on vegetation cover change impact on hydrology suggested that afforestation might decrease total annual Q due to a drastic reduction in Q_{LF} , while as its reverse effect, forest harvesting might increase total annual Q by increasing the

seasonal Q_{LF} . Furthermore, he might find that it is difficult to determine which decrease or increase in Q_{LF} could be caused by the forest harvesting because the reduction in ET could increase soil moisture storage and surface Q , possibly leading to reducing recharge to groundwater storage and the resultant Q_{LF} . The notable insight that emerges from the possibility for reducing Q_{LF} due to forest thinning requires taking into consideration an interaction between soil physics properties and altered ET by thinning as a forest-water resources management.

To find the best forest thinning practice for sustainable water resources from forested catchments, we need more general information on how thinning may affect Q under a large variety of P amount conditions and soil hydrological conditions. As Saksa et al. (2017) partly mentioned, the observational study alone would not be sufficient to detect thinning effects on Q under P shortage conditions and to examine the interaction between soil characteristics and vegetation canopy processes. Using a watershed-scale monthly water balance model, Sun et al. (2015a) succeeded in quantifying the impact of forest thinning practice on water yield over the United States under current and future climate scenarios but only considered the altered ET by a reduction in LAI via thinning. Likewise, Saksa et al.'s (2017) modeling study investigated well the thinning impacts on the water balance of forested headwater basins influenced by the high temporal variability of P . Moreno et al. (2016) further investigated the thinning impacts on hydrological processes affected by the thinning operation-induced changes through direct the canopy process effects and the collateral soil compaction effects in a large-scale basin, with taking into consideration inter- and intra-annual and spatial variations in P . However, it should be noted that despite the well-examined effects of soil characteristics altered by the thinning operations, they did not attempt to examine the relationships between the thinning impacts and variation in soil characteristics possible over forested catchments.

In this study, using a combination of the 8-year hydrological observations, the 100-year stochastic-generated meteorological data, and the semi-process-based rainfall-runoff model, we could demonstrate the combined effects of soil physics parameter m and the altered ET by thinning on Q_{LF} and Q_{IF} in Normal and Dry years, consequently suggesting the optimal thinning intensity corresponding to a variety of soil physics conditions m (Fig. 8). We found that forest thinning would primarily increase Q_{LF} and Q_{IF} at the catchments with larger values of m , i.e., higher water retention capacity. This, in part, is attributed to the fact that at a catchment with low water retention capacity, P_{net} cannot contribute to Q_{LF} and Q_{IF} but to rapid runoff even though a reduction in ET by thinning increases P_{net} . This also suggests that to gain the best hydrological benefit from forest thinning, it is important to refrain from forest treatment actions to lose soil water retention capacity such as soil compaction. Here, we emphasize that assuming the simplified TOP-MODEL that can be optimized with a single parameter, m , can apply to the studied catchment, we can find the best practice of forest thinning for sustainable forested mountain water resources. In short, if m for a subject catchment can be obtained as prior information, the present study can help the ground-level forest and water managers to decide thinning intensity at the catchment and will be further attractive to the policymakers having a mission to improve forest ecosystem services and resilience.

CRedit authorship contribution statement

Hiroki Momiyama: Conceptualization, Methodology, Software, Formal analysis, Writing – original draft. **Tomomi Kumagai:** Conceptualization, Methodology, Writing – review & editing, Supervision, Project administration, Funding acquisition. **Tomohiro Egusa:** Investigation, Data curation, Writing – review & editing.

Declaration of Competing Interest

The authors declare that they have no known competing financial

interests or personal relationships that could have appeared to influence the work reported in this paper.

Acknowledgements

Funding for this work was provided by the Kanagawa Prefectural Government, Japan, as part of the project on 'Forest, soil, and water resource conservation in the western Kanagawa reservoir area.' The authors thank the staff of the Kanagawa Prefectural Government for logistical support to conduct observations throughout the Oborasawa Experimental Watershed (OEW). Members of Forest Biogeosciences Lab (The University of Tokyo) also provided logistical support.

References

- Andréassian, V., 2004. Waters and forests: From historical controversy to scientific debate. *J. Hydrol.* 291, 1–27. <https://doi.org/10.1016/j.jhydrol.2003.12.015>.
- Ao, T.Q., Takeuchi, K., Ishidaira, H., Yoshitani, J., Fukami, K., 2003. Development and application of a new algorithm for automated pit removal for grid DEMs. *Hydrol. Sci. J.* 48, 985–997. <https://doi.org/10.1623/hysj.48.6.985.51423>.
- Baker Jr., M.B., 1986. Effects of ponderosa pine treatments on water yield in Arizona. *Water Resour. Res.* 22, 67–73. <https://doi.org/10.1029/WR022i001p00067>.
- Beven, K.J., Kirkby, M.J., 1979. A physically based, variable contributing area model of basin hydrology. *Hydrol. Sci. Bull.* 24, 43–69. <https://doi.org/10.1080/02626667909491834>.
- Beven, K.J., Lamb, R., Quinn, P., Romanowicz, R., Freer, J., 1995. TOPMODEL. In: Singh, V.P. (Ed.), *Computer models of watershed hydrology*. Water Resource Publications, Colorado, pp. 627–668.
- Bosch, J.M., Hewlett, J.D., 1982. A review of catchment experiments to determine the effect of vegetation changes on water yield and evapotranspiration. *J. Hydrol.* 55 (1–4), 3–23. [https://doi.org/10.1016/0022-1694\(82\)90117-2](https://doi.org/10.1016/0022-1694(82)90117-2).
- Bren, L., Lane, P., Hepworth, G., 2010. Longer-term water use of native eucalyptus forest after logging and regeneration: the Coranderk experiment. *J. Hydrol.* 384 (1–2), 52–64. <https://doi.org/10.1016/j.jhydrol.2010.01.007>.
- Brown, A.E., Zhang, L.u., McMahon, T.A., Western, A.W., Vertessy, R.A., 2005. A review of paired catchment studies for determining changes in water yield resulting from alterations in vegetation. *J. Hydrol.* 310 (1–4), 28–61. <https://doi.org/10.1016/j.jhydrol.2004.12.010>.
- Duan, Q.Y., Gupta, V.K., Sorooshian, S., 1993. Shuffled complex evolution approach for effective and efficient global minimization. *J. Optim. Theory Appl.* 76 (3), 501–521. <https://doi.org/10.1007/BF00939380>.
- Duan, Q., Sorooshian, S., Gupta, V., 1992. Effective and efficient global optimization for conceptual rainfall-runoff models. *Water Resour. Res.* 28 (4), 1015–1031. <https://doi.org/10.1029/91WR02985>.
- Forestry Agency, 2019. *Annual report on trends in forests and forestry fiscal year 2018*. The Ministry of Agriculture, Forestry and Fisheries of Japan, Tokyo.
- Fujime, N., Kumagai, T., Egusa, T., Momiya, H., Uchiyama, Y., 2021. Importance of calibration in determining forest stand transpiration using the thermal dissipation method. *Agric. For. Meteorol.* 301–302, 108356. <https://doi.org/10.1016/j.agrformet.2021.108356>.
- Fujimori, T., 2006. *Forest Ecology: Basics for Sustainable Forest Management*. Zenrinkyou, Tokyo.
- Gabriel, K.R., Neumann, J., 1962. A Markov chain model for daily rainfall occurrence at Tel Aviv. *Q. J. R. Meteorol. Soc.* 88 (375), 90–95. [https://doi.org/10.1002/\(ISSN\)1477-870X10.1002/qj.v88:37510.1002/qj.49708837511](https://doi.org/10.1002/(ISSN)1477-870X10.1002/qj.v88:37510.1002/qj.49708837511).
- Ganatsios, H.P., Tsioras, P.A., Pavlidis, T., 2010. Water yield changes as a result of silvicultural treatments in an oak ecosystem. *For. Ecol. Manage.* 260 (8), 1367–1374. <https://doi.org/10.1016/j.foreco.2010.07.033>.
- Gebhardt, T., Häberle, K.H., Matyssek, R., Schulz, C., Ammer, C., 2014. The more, the better? Water relations of Norway spruce stands after progressive thinning. *Agric. For. Meteorol.* 197, 235–243. <https://doi.org/10.1016/j.agrformet.2014.05.013>.
- Grant, G.E., Tague, C.L., Allen, C.D., 2013. Watering the forest for the trees: an emerging priority for managing water in forest landscapes. *Front. Ecol. Environ.* 11 (6), 314–321. <https://doi.org/10.1890/120209>.
- Hattori, S., Chikaraashi, H., 1988. Effect of thinning on canopy interception in a hinoki stand. *J. Jpn. For. Soc.* 70, 529–533. <https://doi.org/10.11519/jjfs1953.70.12.529>.
- Hawthorne, S.N.D., Lane, P.N.J., Bren, L.J., Sims, N.C., 2013. The long term effects of thinning treatments on vegetation structure and water yield. *For. Ecol. Manage.* 310, 983–993. <https://doi.org/10.1016/j.foreco.2013.09.046>.
- Jarvis, P.G., 1976. The interpretation of the variations in leaf water potential and stomatal conductance found in canopies in the field. *Philos. Trans. R. Soc. B Biol. Sci.* 273, 593–610. <https://doi.org/10.1098/rstb.1976.0035>.
- Jayasuriya, M.D.A., Dunn, G., Benyon, R., O'Shaughnessy, P.J., 1993. Some factors affecting water yield from mountain ash (*Eucalyptus regnans*) dominated forests in south-east Australia. *J. Hydrol.* 150 (2–4), 345–367. [https://doi.org/10.1016/0022-1694\(93\)90116-Q](https://doi.org/10.1016/0022-1694(93)90116-Q).
- Kelliher, F.M., Leuning, R., Raupach, M.R., Schulze, E.-D., 1995. Maximum conductances for evaporation from global vegetation types. *Agric. For. Meteorol.* 73, 1–16. [https://doi.org/10.1016/0168-1923\(94\)02178-M](https://doi.org/10.1016/0168-1923(94)02178-M).
- Komatsu, H., 2020. Modeling evapotranspiration changes with managing Japanese cedar and cypress plantations. *For. Ecol. Manage.* 475, 118395. <https://doi.org/10.1016/j.foreco.2020.118395>.
- Komatsu, H., Shinohara, Y., Nogata, M., Tsuruta, K., Otsuki, K., 2013. Changes in canopy transpiration due to thinning of a *Cryptomeria japonica* plantation. *Hydrol. Res. Lett.* 7 (3), 60–65. <https://doi.org/10.3178/hr.l7.60>.
- Komatsu, H., Tanaka, N., Kume, T., 2007. Do coniferous forests evaporate more water than broad-leaved forests in Japan? *J. Hydrol.* 336 (3–4), 361–375. <https://doi.org/10.1016/j.jhydrol.2007.01.009>.
- Kosugi, K., Katsura, S., Katsuyama, M., Mizuyama, T., 2006. Water flow processes in weathered granitic bedrock and their effects on runoff generation in a small headwater catchment. *Water Resour. Res.* 42, W02414. <https://doi.org/10.1029/2005WR004275>.
- Kubota, T., Tsuboyama, Y., Nobuhiro, T., 2018. Effects of thinning on canopy interception loss, evapotranspiration, and runoff in a small headwater *Chamaecyparis obtusa* catchment in Hitachi Ohta Experimental Watershed in Japan. *Bull. FFPRI* 17, 63–73. <https://doi.org/10.20756/ffpri.17.1.63>.
- Kumagai, T., Katul, G.G., Saitoh, T.M., Sato, Y., Manfroi, O.J., Morooka, T., Ichie, T., Kuraji, K., Suzuki, M., Porporato, A., 2004. Water cycling in a Bornean tropical rain forest under current and projected precipitation scenarios. *Water Resour. Res.* 40, W01104. <https://doi.org/10.1029/2003WR002226>.
- Kumagai, T., Tateishi, M., Miyazawa, Y., Kobayashi, M., Yoshifuji, N., Komatsu, H., Shimizu, T., 2014. Estimation of annual forest evapotranspiration from a coniferous plantation watershed in Japan (1): water use components in Japanese cedar stands. *J. Hydrol.* 508, 66–76. <https://doi.org/10.1016/j.jhydrol.2013.10.047>.
- Kumagai, T., Tateishi, M., Shimizu, T., Otsuki, K., 2008. Transpiration and canopy conductance at two slope positions in a Japanese cedar forest watershed. *Agric. For. Meteorol.* 148 (10), 1444–1455. <https://doi.org/10.1016/j.agrformet.2008.04.010>.
- Lesch, W., Scott, D.F., 1997. The response in water yield to the thinning of *Pinus radiata*, *Pinus patula* and *Eucalyptus grandis* plantations. *For. Ecol. Manage.* 99 (3), 295–307. [https://doi.org/10.1016/S0378-1127\(97\)00045-5](https://doi.org/10.1016/S0378-1127(97)00045-5).
- Linsley, R.K., Kohler, M.A., Paulhus, J.L.H., 1958. *Hydrology for Engineers*. McGraw-Hill, New York.
- Liu, X., Sun, G., Mitra, B., Noormets, A., Gavazzi, M.J., Domec, J.C., Hallema, D.W., Li, J., Fang, Y., King, J.S., McNulty, S.G., 2018. Drought and thinning have limited impacts on evapotranspiration in a managed pine plantation on the southeastern United States coastal plain. *Agric. For. Meteorol.* 262, 14–23. <https://doi.org/10.1016/j.agrformet.2018.06.025>.
- McDonnell, J.J., Evaristo, J., Bladon, K.D., Buttle, J., Creed, I.F., Dymond, S.F., Grant, G., Iroume, A., Jackson, C.R., Jones, J.A., Maness, T., McGuire, K.J., Scott, D.F., Segura, C., Sidle, R.C., Tague, C., 2018. Water sustainability and watershed storage. *Nat. Sustain.* 1 (8), 378–379. <https://doi.org/10.1038/s41893-018-0099-8>.
- McNaughton, K., Black, T., 1973. A study of evapotranspiration from a Douglas fir forest using the energy balance approach. *Water Resour. Res.* 9, 1579–1590. <https://doi.org/10.1016/j.juc.2013.01.005>.
- Ministry of Land, Infrastructure, Transport and Tourism, 2020. Trends in water resources in Japan 2020. Available at: https://www.mlit.go.jp/mizukokudo/mizsei/mizukoku_do_mizsei_tk2_000028.html.
- Momiya, H., Kumagai, T., Egusa, T., 2019. Reproducing monthly evapotranspiration from a coniferous plantation watershed in Japan. *J. For. Res.* 24 (3), 197–200. <https://doi.org/10.1080/13416979.2019.1604606>.
- Moreno, H.A., Gupta, H.V., White, D.D., Sampson, D.A., 2016. Modeling the distributed effects of forest thinning on the long-term water balance and streamflow extremes for a semi-arid basin in the southwestern US. *Hydrol. Earth Syst. Sci.* 20, 1241–1267. <https://doi.org/10.5194/hess-20-1241-2016>.
- Morikawa, Y., Hattori, S., Kiyono, Y., 1986. Transpiration of a 31-year-old *Chamaecyparis obtusa* Endl. stand before and after thinning. *Tree Physiol.* 2 (1–2–3), 105–114. <https://doi.org/10.1093/treephys/2.1-2-3.105>.
- Nanko, K., Onda, Y., Kato, H., Gomi, T., 2016. Immediate change in throughfall spatial distribution and canopy water balance after heavy thinning in a dense mature Japanese cypress plantation. *Ecohydrology* 9 (2), 300–314. <https://doi.org/10.1002/eco.v9.2.1002/eco.1636>.
- Nash, J.E., Sutcliffe, J.V., 1970. River flow forecasting through conceptual models part I — A discussion of principles. *J. Hydrol.* 10 (3), 282–290. [https://doi.org/10.1016/0022-1694\(70\)90255-6](https://doi.org/10.1016/0022-1694(70)90255-6).
- Oda, T., Suzuki, M., Egusa, T., Uchiyama, Y., 2013. Effect of bedrock flow on catchment rainfall-runoff characteristics and the water balance in forested catchments in Tanzawa mountains, Japan. *Hydrol. Process.* 27 (26), 3864–3872. <https://doi.org/10.1002/hyp.v27.26.1002/hyp.9497>.
- Pushpalatha, R., Perrin, C., Le Moine, N., Andréassian, V., 2012. A review of efficiency criteria suitable for evaluating low-flow simulations. *J. Hydrol.* 420–421, 171–182. <https://doi.org/10.1016/j.jhydrol.2011.11.055>.
- Quinn, P., Beven, K., Chevallier, P., Planchon, O., 1991. The prediction of hillslope flow paths for distributed hydrological modelling using digital terrain models. *Hydrol. Process.* 5 (1), 59–79. [https://doi.org/10.1002/\(ISSN\)1099-108510.1002/hyp.v5:110.1002/hyp.3360050106](https://doi.org/10.1002/(ISSN)1099-108510.1002/hyp.v5:110.1002/hyp.3360050106).
- Saksa, P.C., Conklin, M.H., Battles, J.J., Tague, C.L., Bales, R.C., 2017. Forest thinning impacts on the water balance of Sierra Nevada mixed-conifer headwater basins. *Water Resour. Res.* 53 (7), 5364–5381. <https://doi.org/10.1002/2016WR019240>.
- Shinohara, Y., Levina, D.F., Komatsu, H., Nogata, M., Otsuki, K., 2015. Comparative modeling of the effects of intensive thinning on canopy interception loss in a Japanese cedar (*Cryptomeria japonica* D. Don) forest of western Japan. *Agric. For. Meteorol.* 214–215, 148–156. <https://doi.org/10.1016/j.agrformet.2015.08.257>.
- Smakhtin, V.U., 2001. Low flow hydrology: a review. *J. Hydrol.* 240 (3–4), 147–186. [https://doi.org/10.1016/S0022-1694\(00\)00340-1](https://doi.org/10.1016/S0022-1694(00)00340-1).
- Sugawara, M., 1972. *Method of Rainfall-Runoff Analysis*. Kyoritsu Shuppan, Tokyo.
- Sugawara, M., 1995. *Task Model*. In: Singh, V.P. (Ed.), *Computer Models of Watershed Hydrology*. Water Resource Publications, Colorado, pp. 165–214.

- Sun, G., Caldwell, P.V., Menulty, S.G., 2015a. Modelling the potential role of forest thinning in maintaining water supplies under a changing climate across the conterminous United States. *Hydrol. Process.* 29, 5016–5030. <https://doi.org/10.1002/hyp.10469>.
- Sun, X., Onda, Y., Kato, H., Gomi, T., Komatsu, H., 2015b. Effect of strip thinning on rainfall interception in a Japanese cypress plantation. *J. Hydrol.* 525, 607–618. <https://doi.org/10.1016/j.jhydrol.2015.04.023>.
- Sun, X., Onda, Y., Otsuki, K., Kato, H., Gomi, T., 2016. The effect of strip thinning on forest floor evaporation in a Japanese cypress plantation. *Agric. For. Meteorol.* 216, 48–57. <https://doi.org/10.1016/j.agrformet.2014.06.011>.
- Sun, X., Onda, Y., Otsuki, K., Kato, H., Gomi, T., Liu, X., 2017. Change in evapotranspiration partitioning after thinning in a Japanese cypress plantation. *Trees* 31 (5), 1411–1421. <https://doi.org/10.1007/s00468-017-1555-1>.
- Sun, X., Onda, Y., Otsuki, K., Kato, H., Hirata, A., Gomi, T., 2014. The effect of strip thinning on tree transpiration in a Japanese cypress (*Chamaecyparis obtusa* Endl.) plantation. *Agric. For. Meteorol.* 197, 123–135. <https://doi.org/10.1016/j.agrformet.2015.10.006>.
- Suzuki, M., 1985. Evapotranspiration estimates of forested watersheds in Japan using the short-time period water-budget method. *J. Jpn. For. Soc.* 67, 115–125. <https://doi.org/10.11519/jjfs1953.67.4.115>.
- Tadaki, Y., 1976. Biomass of forest, with special reference to the leaf biomass of forests in Japan. *J. Jpn. For. Soc.* 58, 416–423. <https://doi.org/10.11519/jjfs1953.58.11.416>.
- Tani, M., Matsushi, Y., Sayama, T., Sidle, R.C., Kojima, N., 2020. Characterization of vertical unsaturated flow reveals why storm runoff responses can be simulated by simple runoff-storage relationship models. *J. Hydrol.* 588, 124982. <https://doi.org/10.1016/j.jhydrol.2020.124982>.
- Tateishi, M., Xiang, Y., Saito, T., Otsuki, K., Kasahara, T., 2015. Changes in canopy transpiration of Japanese cypress and Japanese cedar plantations because of selective thinning. *Hydrol. Process.* 29, 5088–5097. <https://doi.org/10.1002/hyp.10700>.
- Uchiyama, Y., Nakajima, N., Yokoyama, T., Yamanaka, Y., 2014. Report on hydrological observations by forest conservation project in Ohbora-sawa Watershed in the Tanzawa Mountains. *Bull. Kanagawa Prefect. Nat. Environ. Conserv. Cent.* 12, 17–26.
- Wilks, D.S., Wilby, R.L., 1999. The weather generation game: a review of stochastic weather models. *Prog. Phys. Geogr. Earth Environ.* 23 (3), 329–357. <https://doi.org/10.1177/030913339902300302>.
- Yilmaz, K.K., Gupta, H.V., Wagener, T., 2008. A process-based diagnostic approach to model evaluation: Application to the NWS distributed hydrologic model. *Water Resour. Res.* 44, W09417. <https://doi.org/10.1029/2007WR006716>.
- Yokoo, Y., Sivapalan, M., 2011. Towards reconstruction of the flow duration curve: development of a conceptual framework with a physical basis. *Hydrol. Earth Syst. Sci.* 15, 2805–2819. <https://doi.org/10.5194/hess-15-2805-2011>.
- Yokoyama, T., Uchiyama, Y., Mitsuhashi, M., 2014. Study on hydrogeological features of Ohbora-sawa watershed in the eastern Tanzawa mountains. *Bull. Kanagawa Prefect. Nat. Environ. Conserv. Cent.* 12, 1–16.
- Yokoyama, T., Uchiyama, Y., Satou, S., Yamane, M., 2013. Hydrogeological features of 4 experimental watersheds in the water resources protection area. *Bull. Kanagawa Prefect. Nat. Environ. Conserv. Cent.* 10, 203–214.
- Zhang, Y., Deng, L., Yan, W., Shangguan, Z., 2016. Interaction of soil water storage dynamics and long-term natural vegetation succession on the Loess Plateau, China. *Catena* 137, 52–60. <https://doi.org/10.1016/j.catena.2015.08.016>.